RAPID COMMUNICATIONS IN MASS SPECTROMETRY
Rapid Commun. Mass Spectrom. 2005; **19**: 1031–1040
Published online in Wiley InterScience (www.interscience.wiley.com). DOI: 10.1002/rcm.1887

RCM

Interactions of platinum(II) complexes with sulfur-containing peptides studied by electrospray ionization mass spectrometry and tandem mass spectrometry

Ren Miao, Gaosheng Yang, Yi Miao, Yuhua Mei, Jin Hong, Chunmei Zhao and Longgen Zhu*

State Key Laboratory of Coordination Chemistry, Coordination Chemistry Institute, Nanjing University, Nanjing, 210093, China

Received 22 December 2004; Revised 21 February 2005; Accepted 22 February 2005

Reactions of two platinum(II) complexes, *cis*-$[Pt(NH_3)_2(H_2O)_2]^{2+}$ (Pt1) and *cis*-$[Pt(en)(H_2O)_2]^{2+}$ (Pt2), with several sulfur-containing peptides, have been investigated by electrospray ionization mass spectrometry (ESI-MS) and tandem mass spectrometry (MS/MS). The species produced in the reactions were detected with ESI-MS, and MS/MS analysis was performed to probe structural information. Collision-induced dissociation revealed different dissociation pathways for the main reaction products of the two platinum(II) complexes with the same peptides. The major difference is the prominent loss of ammonia ligand for complexes of Pt1 due to the strong *trans* effect of sulfur, whereas the loss of ethylenediamine (en) ligand from Pt2 complexes is less favored, reflecting the chelating effect of the bidentate ligand. Despite the differences in dissociation patterns, Pt1 and Pt2, in general, form structurally similar complexes with the same peptides. In the reactions with Met-Arg-Phe-Ala they both produce a N,S-chelate ring through the N-terminal NH_2 and sulfur of the Met residue, and in the reactions with Ac-Met-Ala-Ser they bind to the sulfur of Met and deprotonate an amide nitrogen upstream from the anchor site. Both of them are able to promote hydrolysis of the peptides. In reactions with glutathione they both form four-membered Pt_2S_2 rings and Pt-S-Pt bonding through the bridging thiolate ligand, although the reaction rate is much slower for Pt2 due to steric hindrance of the en ligand.

Platinum chemistry has considerable importance in medicine and biochemistry. Cisplatin (*cis*-$[PtCl_2(NH_3)_2]$)[1] and carboplatin ($[Pt(CBDCA\text{-}O,O')(NH_3)_2]$,[2] where CBDCA is cyclobutane-1,1-dicarboxylate, have long been recognized and used as anticancer drugs. Attack on DNA is suggested to be responsible for their antitumor activity, while platinum complexes can also interact with many other biomolecules, especially those containing sulfur for which Pt has a very high affinity. Examples of sulfur-containing biomolecules include amino acids such as cysteine and methionine, peptides such as glutathione, and proteins such as metallothioneins, and many others. Interactions of platinum complexes with sulfur-containing molecules are thought to be responsible for a variety of biological effects, such as inactivation of platinum(II) complexes, development of cellular resistance to platinum, and toxic side effects such as nephrotoxicity.[3]

**Correspondence to*: L. Zhu, State Key Laboratory of Coordination Chemistry, Coordination Chemistry Institute, Nanjing University, Nanjing, 210093, China.
E-mail: zhulg@public1.ptt.js.cn
Contract/grant sponsor: National Science Foundation of China; contract/grant numbers: 20271027 and 20231010.

In the last decade complexes of platinum(II), e.g. *cis*-$[Pt(en)(H_2O)_2]^{2+}$ and *cis*-$[Pt(NH_3)_2(H_2O)_2]^{2+}$, have been found to be new efficient reagents for selective hydrolytic cleavage of peptides and proteins.[4–6] These platinum(II) complexes first anchor to specific side chains, e.g. the sulfur atom of methionine or cysteine, and then regioselectively cleave amide bonds in the vicinity under mild experimental conditions.

Many studies of the interactions of platinum(II) complexes with peptides and proteins have been conducted. Most rely mainly on nuclear magnetic resonance (NMR) spectroscopy, especially ^{195}Pt and ^{15}N NMR spectroscopy, high-performance liquid chromatography (HPLC), and other experimental methods. Nevertheless, as one of the effective analytical methods in investigations of both solution- and gas-phase chemistry, electrospray ionization mass spectrometry (ESI-MS) has scarcely been used as a major analytical tool in research into reactions of platinum(II) complexes with peptides and proteins.[6,7]

In recent years ESI-MS has had a profound impact on various areas of chemical analysis. ESI-MS provides a 'soft' method to transfer pre-existing ions from the solution phase into the gas phase with minimal fragmentation. More

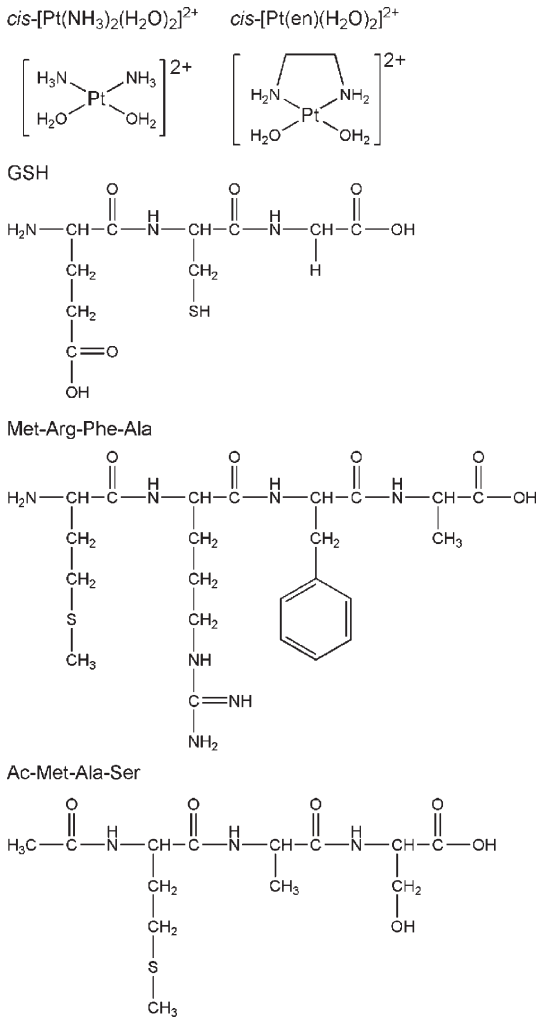

Scheme 1. Platinum(II) complexes (Pt1 and Pt2) and the sulfur-containing peptides investigated in this study.

importantly, the structures and the magnitude of their charges appear to generally remain intact, permitting good correlations between solution-phase ions and gas-phase ions.[8] Collision-induced dissociation (CID) can be utilized to obtain structural information. ESI-MS/MS has been widely used in bioanalytical chemistry,[9–13] inorganic chemistry[14] and organometallic chemistry.[14–16]

In this work two platinum complexes which have been found to be effective artificial metallopeptidases, i.e. *cis*-$[Pt(NH_3)_2(H_2O)_2]^{2+}$ (Pt1) and *cis*-$[Pt(en)(H_2O)_2]^{2+}$ (Pt2), were investigated with respect to their interactions with three peptides with different sulfur-containing side chains, namely, glutathione GSH (containing a thiol side chain), Met-Arg-Phe-Ala (containing a thioether side chain and a terminal amino group), and Ac-Met-Ala-Ser (containing a thioether side chain and an acetylated terminal amino group), with the intention of investigating their hydrolysis behavior (see Scheme 1). In order to probe the structures of the reaction products, tandem mass spectrometry (MS/MS) and multi-stage tandem mass spectrometry (MS^n) were used. We demonstrate in this study that ESI-MS can be used as an effective analytical tool for studying the interactions of platinum(II) complexes with peptides or even proteins, and that MS/MS can provide valuable structural information about the species formed in solution.

EXPERIMENTAL

cis-$Pt(en)Cl_2$ was purchased from Aldrich, glutathione (GSH) and Met-Ala-Ser (MAS) were purchased from Sigma, and Ac-Met-Ala-Ser (AcMAS) was obtained from MAS by a published procedure;[5] Met-Arg-Phe-Ala (MRFA) was purchased from Research Plus, Inc. *cis*-$Pt(NH_3)_2Cl_2$ was synthesized according to a published procedure.[17] $AgNO_3$ of reagent grade was used. Double-distilled water was used in all preparations.

Solutions of *cis*-$[Pt(NH_3)_2(H_2O)_2]^{2+}$ (Pt1) and *cis*-$[Pt(en)(H_2O)_2]^{2+}$ (Pt2) were obtained by mixing each of *cis*-$Pt(NH_3)_2Cl_2$ and *cis*-$Pt(en)Cl_2$ with two equivalent amounts of $AgNO_3$ in water, and stirring overnight in the dark. The white AgCl precipitate was removed by centrifugation to obtain 50 mM solutions of Pt1 and Pt2. A typical experimental procedure was to mix Pt1 (50 mM) or Pt2 (50 mM) with an aqueous peptide solution (50 mM) in a molar ratio of 1:1; the mixed solution was acidified with HBF_4 to adjust the solution pH to ca. 2.0, and the mixture was incubated at 310 K in preparation for ESI-MS measurements which were conducted at ca. 10 min intervals.

ESI mass spectra and tandem mass spectra were recorded using a Finnigan-MAT LCQ ion-trap mass spectrometer in the positive ionization mode. Typically, ~1–2 μL of the mixture solution, prepared as described above, was transported into the ESI-MS instrument by 50% of aqueous methanol at a flow rate of 200 μL/min. Experimental operating conditions were optimized for maximum intensity of the platinum(II) complex ion. The ESI instrument parameters were as follows: the ESI spray needle voltage was +4.5 kV, N_2 sheath gas flow was 35 units (arbitrary units), and the capillary desolvation temperature was 200°C. Helium gas was directly admitted into the ion trap and used both as the damping gas to improve trapping efficiency and as the collision gas in the CID experiments. Automatic gain control (AGC) was turned on to control the ion injection (AGC target values were set to 5×10^7 for full-scan MS and 2×10^7 for MS^n); maximum injection time was set to 400 ms. To induce collisional activation the relative collision energy was controlled between 20–40% of maximum, depending on the precursor ion and the MS^n stage. MS/MS and MS^n experiments were performed using an isolation width of 6 Th for the precursor ions in order to allow the Pt isotopic signature to be observed in the MS/MS spectra.

RESULTS AND DISCUSSION

ESI mass spectra of Pt1 and Pt2

The ESI mass spectra for Pt1 and Pt2 are shown in Fig. 1. Pt1 generated two prominent ion clusters, at *m/z* 263.0–267.0 and 294.8–298.8. The isotope distribution pattern of the cluster at *m/z* 263.0–267.0 is shown in the inset of Fig. 1(A) and indicates that this ion is singly charged based on the spacing of 1 Th between peaks, and contains one Pt atom. This ion is attributed to $[Pt(NH_3)_2(H_2O)(OH)]^+$; the relative abundances of isotope peaks match the expected values very well, i.e., *m/z* 263.0

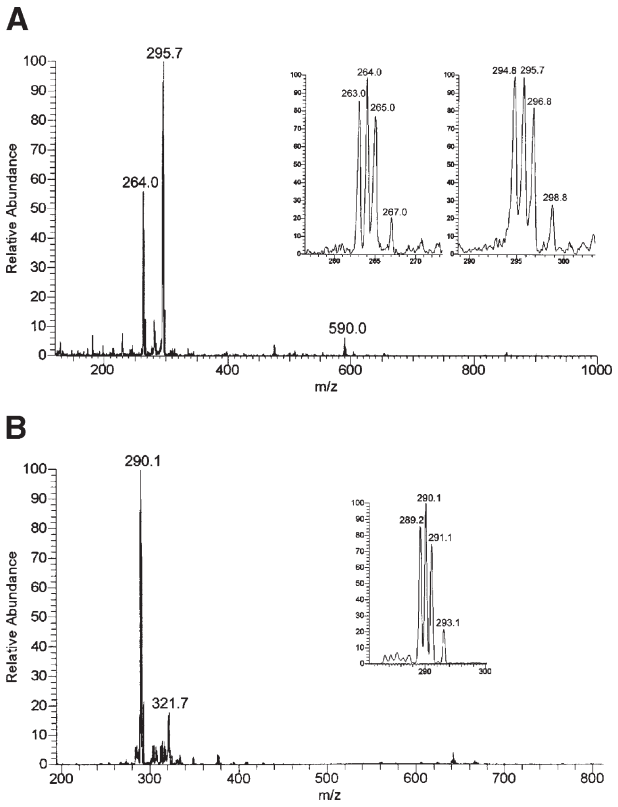

Figure 1. ESI mass spectra recorded for Pt1 (A) and Pt2 (B).

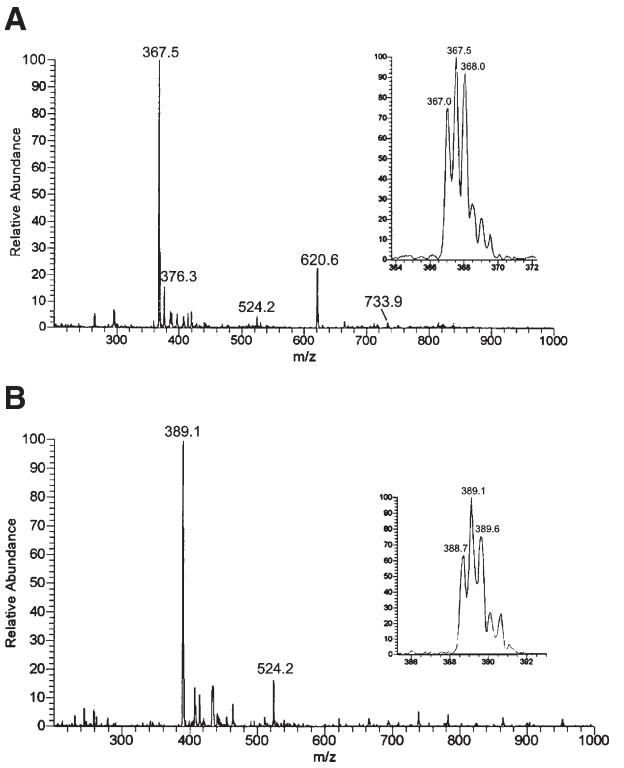

Figure 2. ESI mass spectra collected after 1 h in reaction of (A) Pt1 and (B) Pt2 with MRFA.

~32%, *m/z* 264.0 ~34%, *m/z* 265.0 ~25%, and *m/z* 267.0 ~7%. The *m/z* values for the second major ion cluster are consistent with the mass of the adduct of $[Pt(NH_3)_2(H_2O)(OH)]^+$ with one methanol molecule, i.e. $[Pt(NH_3)_2(H_2O)(OH)]\,(CH_3OH)^+$. This identification was confirmed by a CID experiment in which the *m/z* 294.8–298.8 cluster was selected as precursor, when the most prominent fragment ion produced was *m/z* 263.0–267.0 (spectrum not shown), as expected for $[Pt(NH_3)_2(H_2O)(OH)]^+$.

For purposes of clarity in the discussion below, the *m/z* values quoted for ions containing Pt refer to ^{195}Pt only. The minor peak at *m/z* 590.0 in Fig. 1(A) corresponds to a singly charged species containing two Pt atoms, based on its isotope distribution (spectrum not shown), and may be attributed to a dimer of $[Pt(NH_3)_2(H_2O)(OH)]\,(CH_3OH)^+$, namely, $\{[Pt(NH_3)_2(H_2O)(OH)(CH_3OH)]_2-H\}^+$.

As shown in Fig. 1(B), Pt2 produced only one prominent ion at *m/z* 290.1. Similarly, the isotope distribution pattern and the *m/z* values in the ion cluster allow assignment of this ion to $[Pt(en)(H_2O)(OH)]^+$. Compared to Pt1, the relative abundance of the methanol adduct of $[Pt(en)(H_2O)(OH)]^+$, at *m/z* 321.7, is relatively low.

Reactions of Pt1 and Pt2 with Met-Arg-Phe-Ala (MRFA)

After mixing solutions of Pt1 and MRFA in a molar ratio of 1:1 as described above, mass spectra were collected at 10 min intervals. The relative abundance of the protonated reactant MRFA (*m/z* 524.2) decreased with time, while that of the product at *m/z* 367.5 increased. The spectrum recorded after 1 h is shown in Fig. 2(A); it is apparent from this spectrum that the ion at *m/z* 367.5 has become the major species in the mixture solution after 1 h, and underwent only a slight change with longer reaction time. As shown in the inset of Fig. 2(A), the isotope peaks separated by 0.5 Th indicate that the ion at *m/z* 367.5 is doubly charged, and can thus be tentatively attributed to $(MRFA+Pt+NH_3)^{2+}$.

In order to probe the structure of this ion at *m/z* 367.5, $(MRFA+Pt+NH_3)^{2+}$, CID-MS/MS analysis was performed. The CID-MS/MS spectral data (mass/charge ratios, assigned elemental compositions, relative abundances normalized to the base peak, and assignment as a peptide fragment ion) are summarized in Table 1. The fragment ion at *m/z* 359.2 corresponds to loss of 17 u from the precursor, and is thus attributed to loss of ammonia, i.e. $(MRFA+Pt)^{2+}$. The ion at *m/z* 322.9 is attributed to $(c_3+H+Pt)^{2+}$, employing the conventional nomenclature for peptide fragments,[18,19] and the predominant ion at *m/z* 300.5 is attributed to $(a_3-H+Pt)^{2+}$. The fact that all fragment ions contain the N-terminus suggests that Pt(II) binds to the N-terminal groups. We propose that Pt(II) is likely to be coordinated to both the sulfur atom of the thioether and the terminal NH_2 group, considering the strong coordination ability of these functional groups. It is well accepted that Pt(II) has a strong tendency to be coordinated by four ligands to complete its square-planar coordination mode. Therefore, in addition to the ammonia, sulfur and terminal NH_2 ligands, the fourth coordination site of platinum(II) is probably occupied by either the carbonyl oxygen of the Met residue or the amide nitrogen of the Arg residue; this is similar to palladium(II) complexes[20,21] for which a fused six-membered and five-membered ring structure has been proposed based on

Table 1. MS/MS analysis of the precursor ions $(MRFA+Pt+NH_3)^{2+}$ (*m/z* 367.5) and $(MRFA+Pt+en)^{2+}$ (*m/z* 389.1)

Precursor	Fragment *m/z*	Elemental composition	Relative abundance (%)	Assignment
$(MRFA+Pt+NH_3)^{2+}$	300.5	$[C_{19}H_{30}N_6O_2SPt]^{2+}$	100	$(a_3-H+Pt)^{2+}$
	322.9	$[C_{20}H_{33}N_7O_3SPt]^{2+}$	11	$(c_3+H+Pt)^{2+}$
	359.2	$[C_{23}H_{37}N_7O_5SPt]^{2+}$	6	$(MRFA+Pt)^{2+}$
$(MRFA+Pt+en)^{2+}$	300.5	$[C_{19}H_{30}N_6O_2SPt]^{2+}$	20	$(a_3-H+Pt)^{2+}$
	330.6	$[C_{21}H_{38}N_8O_2SPt]^{2+}$	100	$(a_3-H+Pt+en)^{2+}$
	344.5	$[C_{22}H_{38}N_8O_3SPt]^{2+}$	36	$(b_3-H+Pt+en)^{2+}$
	353.4	$[C_{22}H_{41}N_9O_3SPt]^{2+}$	28	$(c_3+H+Pt+en)^{2+}$

ESI-MS data. According to these earlier studies,[20,21] the Met-Arg bond in the peptide would be activated towards hydrolysis if the carbonyl oxygen of the Met residue coordinates to Pt(II). However, no hydrolysis of the peptide was observed in this study even when the solution of Pt1 and MRFA was allowed to stand for 1 week at 310 K, which suggests that the carbonyl oxygen of the Met residue is unlikely to serve as the fourth coordinating group; instead, the amide nitrogen of the Arg residue likely coordinates to Pt(II). Coordination of divalent metal ions to an amide nitrogen is always accompanied by deprotonation of the amide nitrogen.[22,23] The peak at *m/z* 733.9 in Fig. 2(A), which is assigned as the species $(MRFA-H+Pt+NH_3)^+$, is thus consistent with the coordination of the amide nitrogen of the Arg residue to Pt(II). Due to the basicity of the Arg side chain, a much more intense peak observed at *m/z* 367.5 is a doubly charged Arg-protonated species assigned as $(MRFA+Pt+NH_3)^{2+}$, and a proposed structure of this complex ion is shown in Scheme 2 (top).

Note that one ammonia ligand was substituted during the reaction. This is consistent with the known fact that the strong *trans* effect of sulfur makes the loss of the ammonia facile; the coordination ability of the deprotonated amide nitrogen serves as another driving force. The ion at *m/z* 376.3 (Fig. 2(A)) is attributed to $(MRFA+Pt+2NH_3)^{2+}$, in which two ammonia molecules remain coordinated to Pt(II). This ion appears to be a precursor for further substitution of ammonia by the amide nitrogen of the Arg residue; the second ammonia ligand seems stable under the experimental conditions. However, it was found that none of the fragment ions generated from the precursor at *m/z* 367.5 contained the second ammonia, which indicates that the second ammonia is readily lost under CID conditions.

Another significant ion in Fig. 2(A) is at *m/z* 620.6; this is also doubly charged based on its isotope distribution pattern (data not shown), and is attributed to $(Pt+2MRFA)^{2+}$ in which two MRFA molecules coordinate to Pt(II), each via S,N-chelation.

The reaction of Pt2 with MRFA proceeded similarly to that of Pt1. The major ion observed at *m/z* 389.1 became the predominant peak about 1 h after mixing the solutions, as shown in Fig. 2(B) and the spectra remained almost unchanged with longer reaction times. Similarly, the ion at *m/z* 389.1 was also doubly charged (see inset of Fig. 2(B)), and is thus attributed to $(MRFA+Pt+en)^{2+}$. The CID analysis of this ion, as shown in Table 1, suggests that Pt(II) is again coordinated to the N-terminal group of the Met residue, since no observed fragment ions contain the C-terminus. The fragment ions at *m/z* 353.4, 344.5 and 330.6 are attributed to $(c_3+H+Pt+en)^{2+}$, $(b_3-H+Pt+en)^{2+}$, and $(a_3-H+Pt+en)^{2+}$, respectively. Thus the precursor ion at *m/z* 389.1 is postulated to have a structure in which Pt(II) is coordinated to sulfur and terminal NH_2, as shown in Scheme 2 (bottom). The fragment ion at *m/z* 300.5 may result from loss of the en ligand, i.e. $(a_3-H+Pt)^{2+}$.

Platinum complexes with amino acids in solution have been studied for decades, and their structures have been characterized in detail. It was concluded that the thermodynamically most stable bonding mode for sulfur-containing amino acids, i.e. methionine or cysteine, is N,S-chelation.[24] Thus the structures proposed here for the product ion species, deduced from ESI-MS and CID spectra, are generally consistent with those derived from other experimental methods.

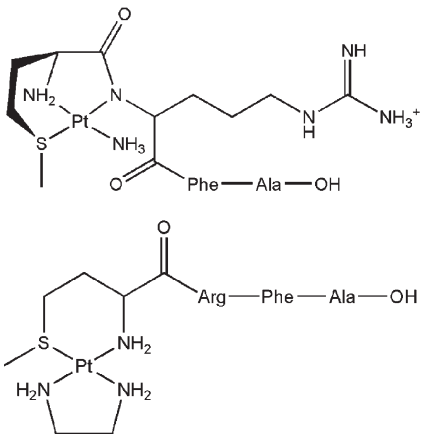

Scheme 2. Structures proposed for $(MRFA+Pt+NH_3)^{2+}$ (top) and $(MRFA+Pt+en)^{2+}$ (bottom).

Reactions of Pt1 and Pt2 with Ac-Met-Ala-Ser (AcMAS)

The results described in the preceding section indicate that Pt1 and Pt2 are unable to cleave peptides when the N-terminal NH_2 is available for coordination. The major reaction product has a N,S-chelation structure and no active site for cleavage. Therefore, acetylated Met-Ala-Ser (AcMAS) was investigated with respect to its binding mode with Pt(II) and its resulting hydrolysis behavior.

After mixing the solutions containing Pt1 and AcMAS in a molar ratio of 1:1, mass spectra were recorded every 10 min. Two species appeared at *m/z* 576.9 and 418.7 after 10 min; at early reaction times (within ca. 0.5 h), the species at *m/z* 576.9

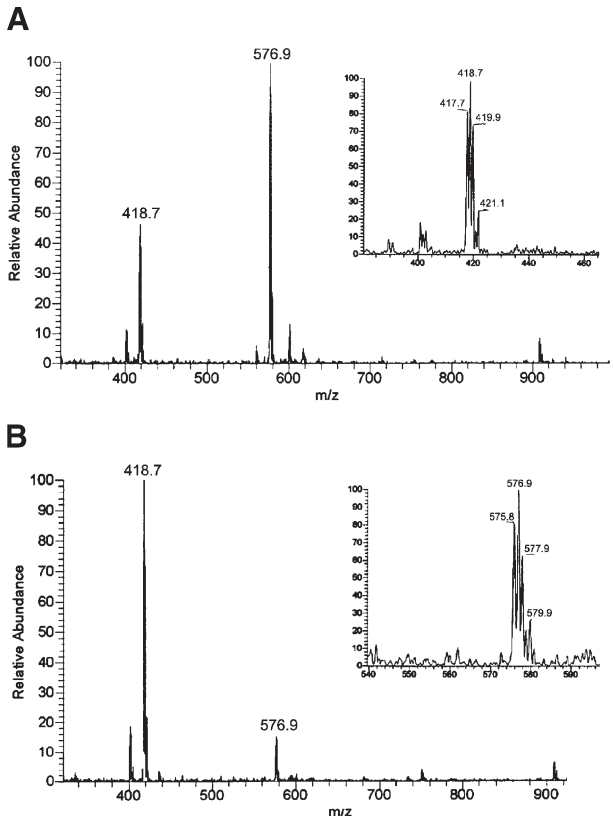

Figure 3. ESI mass spectra collected after (A) ca. 30 min and (B) ca. 2 h, for reaction of Pt1 with AcMAS.

was relatively more abundant, but at longer reaction times (after ca. 2.5 h) the ion at *m/z* 418.7 became the predominant species and the ion at *m/z* 576.9 became almost indiscernible. The mass spectra recorded after ca. 30 min and 2 h are shown in Fig. 3. The isotopic distribution patterns (see insets in Figs. 3(A) and 3(B)) of these species indicate that both of them are singly charged ions containing one Pt atom. These two ions are attributed to $(AcMAS–H+Pt+2NH_3)^+$ for *m/z* 576.9, and $(AcMet–H+Pt+2NH_3)^+$ for *m/z* 418.7, a hydrolysis product of AcMAS.

$(AcMAS–H+Pt+2NH_3)^+$ (*m/z* 576.9) is proposed to have undergone deprotonation at the amide nitrogen of the Met residue, considering the known tendency of Pt(II) to deprotonate amide nitrogens and the observation that deprotonation of amide nitrogen is common in both gas and solution phases for peptides cationized by divalent transition-metal ions.[22,23] In the case of $(AcMet–H+Pt+2NH_3)^+$ (*m/z* 418.7) the deprotonation may take place at either the carboxylic group or at the amide nitrogen of methionine.

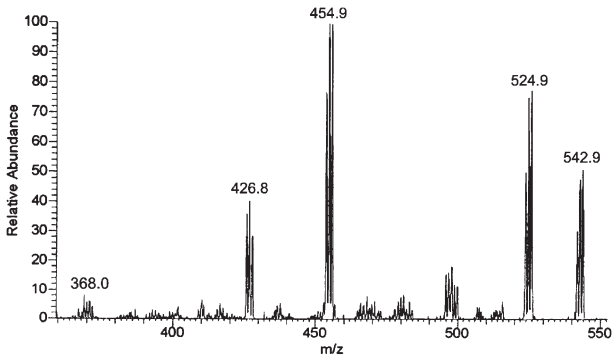

Figure 4. MS^3 spectrum of the precursor $(AcMAS–H+Pt+2NH_3)^+$ (*m/z* 576.9) via the intermediate ion $(AcMAS–H+Pt+NH_3)^+$ (*m/z* 559.9).

CID experiments were performed for these two precursor ions; the fragment ion data are summarized in Table 2. The predominant fragment ions at *m/z* 559.9 and 542.9 for $(AcMAS–H+Pt+2NH_3)^+$ as precursor correspond to losses of one and two molecules of ammonia, respectively; subsequent loss of one water molecule gives rise to the fragment ion at *m/z* 524.9. The fragment ion at *m/z* 454.9 has two possible assignments with the same *m/z* ratio that cannot be distinguished by low-resolution MS/MS data, i.e. $(b_2–2H+Pt+NH_3)^+$ or $(c_2+Pt)^+$; therefore, MS^3 experiments were conducted to probe its structure. The fragment ions at *m/z* 559.9 and 542.9 were selected as the intermediate ions for MS^3 experiments. The MS^3 spectrum of $(AcMAS–H+Pt+2NH_3)^+$ (*m/z* 576.9) as precursor ion via $(AcMAS–H+Pt+NH_3)^+$ (*m/z* 559.9) as intermediate contains an abundant fragment ion at *m/z* 454.9 (see Fig. 4), whereas the MS^3 spectrum via $(AcMAS–H+Pt)^+$ (*m/z* 542.9) as intermediate does not (spectrum not shown). This indicates that the ion at *m/z* 454.9 should be assigned as $(b_2–2H+Pt+NH_3)^+$. The ion at *m/z* 426.8 (28 u loss, i.e. CO, from *m/z* 454.9) is then attributed to $(a_2–2H+Pt+NH_3)^+$. The fragment ion at *m/z* 368.0 is attributed to $(b_1–2H+Pt)^{2+}$, consistent with the assumption that Pt(II) is coordinated to the acetylated terminal nitrogen. Moreover, by taking into account the stability of six-membered chelate rings, the structure of the precursor ion $(AcMAS–H+Pt+2NH_3)^+$ is proposed to be that shown in Scheme 3 (left), with deprotonation occurring at the acetylated terminal nitrogen; a similar structure has been proposed previously.[4,25]

The CID spectral information for the precursor $(AcMet–H+Pt+2NH_3)^+$ is shown in Table 2. The only significant fragment ion at *m/z* 401.9 corresponds to loss of 17 u (presumably ammonia) from the precursor ion, and is thus

Table 2. MS/MS analysis of the precursor ions $(AcMAS–H+Pt+2NH_3)^+$ (*m/z* 576.9) and $(AcMet–H+Pt+2NH_3)^+$ (*m/z* 418.7)

Precursor	Fragment *m/z*	Elemental composition	Relative abundance (%)	Assignment
$(AcMAS–H+Pt+2NH_3)^+$	454.9	$[C_{10}H_{18}N_3O_3SPt]^+$	20	$(b_2–2H+Pt+NH_3)^+$
	524.9	$[C_{13}H_{20}N_3O_5SPt]^+$	11	$(AcMAS–H+Pt–H_2O)^+$
	542.9	$[C_{13}H_{22}N_3O_6SPt]^+$	58	$(AcMAS–H+Pt)^+$
	559.9	$[C_{13}H_{25}N_4O_6SPt]^+$	100	$(AcMAS–H+Pt+NH_3)^+$
$(AcMet–H+Pt+2NH_3)^+$	401.9	$[C_7H_{15}N_2O_3SPt]^+$	100	$(AcMet–H+Pt+NH_3)^+$

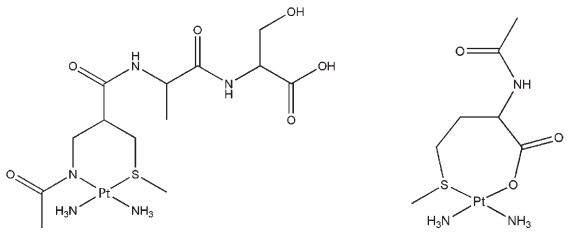

Scheme 3. Structures proposed for (AcMAS−H+Pt+$2NH_3$)$^+$ (left) and (AcMet−H+Pt+$2NH_3$)$^+$ (right).

attributed to (AcMet−H+Pt+NH_3)$^+$. A MS^3 experiment with *m/z* 401.9 as the intermediate ion produced an abundant fragment ion at *m/z* 385.0 (spectrum not shown), which corresponds to loss of the second ammonia. The absence of any fragment ions corresponding to fragmentation of the peptide backbone suggests existence of a stable chelate structure. It seems likely that this species has a S,O-chelation structure, such as that shown in Scheme 3 (right), which prevents further fragmentation of the peptide backbone. A similar solution-phase structure derived from NMR spectroscopy has been reported.[26]

It is noted that loss of the second ammonia by CID was less favored, i.e. the bond between the second ammonia and Pt(II) exhibits moderate stability while loss of the first ammonia is facile due to the strong *trans* effect of the sulfur atom. The *trans* effect of ligands in square-planar complexes has been shown to be an important factor controlling the dissociation patterns in gas-phase fragmentations.[27]

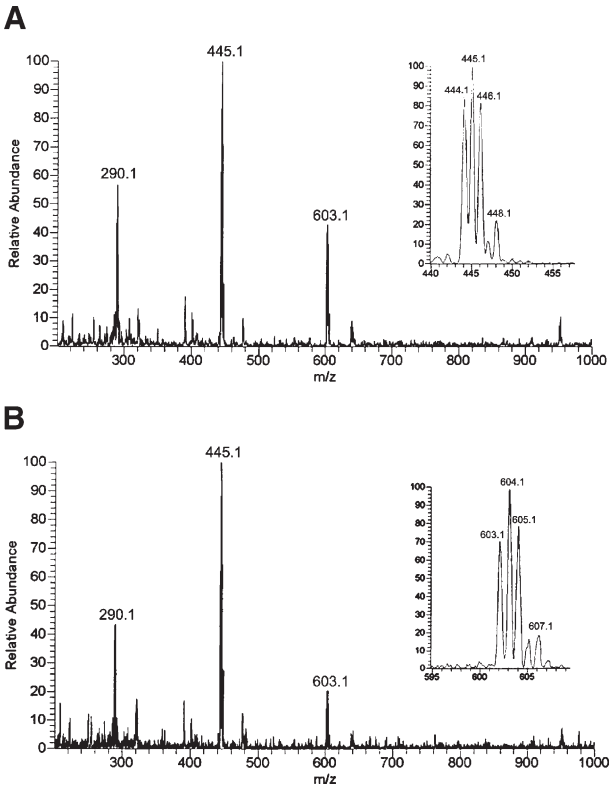

Figure 5. ESI mass spectra collected after (A) ca. 30 min and (B) ca. 1 h, in reaction of Pt2 with AcMAS.

Reaction of Pt2 with AcMAS proceeded similarly. The hydrolysis product at *m/z* 445.1 appeared after 10 min, while a species at *m/z* 603.1 played a major role at early reaction times. At longer reaction times the species at *m/z* 445.1 became dominant. The ESI mass spectra collected after ca. 30 min and ca. 1 h are shown in Fig. 5. The two major product species are assigned as (AcMAS−H+Pt+en)$^+$ (*m/z* 603.1) and (AcMet−H+Pt+en)$^+$ (*m/z* 445.1).

The CID spectral data of the precursor (AcMAS−H+Pt+en)$^+$ (*m/z* 603.1) are summarized in Table 3. Loss of water gives rise to *m/z* 585.0, and fragment ions at *m/z* 514.9, 498.0, and 470.0 are attributed to (c_2+Pt+en)$^+$, (b_2−H+Pt+en)$^+$, and (a_2−H+Pt+en)$^+$, respectively. The fragment ion at *m/z* 543.0 corresponds to loss of 60 u from the precursor, corresponding to the mass of the ligand ethylenediamine (en), so this ion is assigned as (AcMAS+Pt)$^+$. The loss of en is further confirmed by observation of *m/z* 455.0, which is attributed to (c_2+Pt)$^+$. The fragment ion at *m/z* 427.0 is attributed to (b_1−H+Pt+en)$^+$. It is thus reasonable to propose that Pt(II) is coordinated to the deprotonated amide nitrogen of the Met residue to form the structure shown on the left-hand side of Scheme 4, similar to the structure of the corresponding Pt1 complex.

The CID spectrum of (AcMet−H+Pt+en)$^+$ (Table 3) is significantly different from that of (AcMet−H+Pt+$2NH_3$)$^+$ (Table 2), and this may indicate a different bonding mode. The fragment ion at *m/z* 426.9 corresponds to loss of a water molecule and that at *m/z* 401.0 corresponds to loss of CO_2. Such losses may indicate that the C-terminus remains uncoordinated and that the deprotonation occurs at the acetylated N-termial nitrogen.[22] Thus the precursor ion (AcMet−H+Pt+en)$^+$ is proposed to have the structure shown on the right-hand side of Scheme 4. A similar structure deduced from NMR and other analytical methods has also been reported elsewhere.[26] The fragment ion at *m/z* 385.0 corresponds to loss of 60 u, i.e. the en ligand. The fragment ion at *m/z* 302.0 is observed in CID spectra of both *m/z* 603.1 and 455.1 ions; this species may correspond to further fragmentation of the peptide backbone, and we tentatively attribute this ion to (Pt+en+SCH_3)$^+$. This observation may indicate that sulfur is the intrinsic anchor site for Pt(II), and that the Pt−S bond has rather high stability in such complexes. A more rigorous investigation of the nature of this fragment ion using other methionine-containing peptides or isotope-labeled peptides will be discussed in a future report.

It is interesting that the bonding modes of complexes of Pt1 and Pt2 with AcMet are different. This may arise from the ring strain imposed by the bidentate en ligand in Pt2. The en ligand coordinates to Pt(II) through its two NH_2 groups to form a five-membered chelate ring; therefore, when another chelate ring is formed at the remaining two coordination sites of Pt(II) in the complexes with sulfur-containing peptides, a six-membered chelate ring may be favored over a seven-membered ring, as suggested by the present observations.

Reaction of Pt1 and Pt2 with GSH

The results discussed in the preceding sections suggest that the sulfur in a thioether group serves as the intrinsic anchor site for platinum attachment to peptides. The sulfur in a thiol group is expected to be an even stronger anchor site for 'soft'

Table 3. MS/MS analysis of the precursor $(AcMAS-H+Pt+en)^+$ (*m/z* 603.1) and $(Ac\ Met-H+Pt+en)^+$ (*m/z* 445.1)

Precursor	Fragment *m/z*	Elemental composition	Relative abundance (%)	Assignment
$(AcMAS-H+Pt+en)^+$	302.0	$[C_3H_{11}N_2SPt]^+$	12	$(Pt+en+SCH_3)^+$
	427.0	$[C_9H_{18}N_3O_2SPt]^+$	34	$(b_1-H+Pt+en)^+$
	455.0	$[C_{10}H_{18}N_3O_3SPt]^+$	34	$(c_2+Pt)^+$
	470.0	$[C_{11}H_{23}N_4O_2SPt]^+$	67	$(a_2-H+Pt+en)^+$
	498.0	$[C_{12}H_{23}N_4O_3SPt]^+$	100	$(b_2-H+Pt+en)^+$
	514.9	$[C_{12}H_{26}N_5O_3SPt]^+$	25	$(c_2+Pt+en)^+$
	543.0	$[C_{13}H_{22}N_3O_6SPt]^+$	60	$(AcMAS+Pt)^+$
	585.0	$[C_{15}H_{28}N_5O_5SPt]^+$	17	$(AcMAS-H+Pt+en-H_2O)^+$
$(Ac\ Met-H+Pt+en)^+$	302.0	$[C_3H_{11}N_2SPt]^+$	100	$(Pt+en+SCH_3)^+$
	385.0	$[C_7H_{12}NO_3SPt]^+$	42	$(AcMet-H+Pt)^+$
	401.0	$[C_8H_{20}N_3OSPt]^+$	25	$(AcMet-H+Pt+en-CO_2)^+$
	426.9	$[C_9H_{18}N_3O_2SPt]^+$	48	$(AcMet-H+Pt+en-H_2O)^+$

metal ions, including platinum. We thus extended this investigation to the reaction of Pt1 and Pt2 with GSH, which contains a thiol group in a side chain.

After mixing solutions containing Pt1 and GSH in a 1:1 molar ratio, ESI-MS spectra were collected every 10 min; the mass spectrum recorded after 10 min is shown in Fig. 6(A). Protonated GSH (*m/z* 308.0) remains as the predominant ion, and the major product ion at *m/z* 534.9 is a doubly charged species that contains two Pt atoms based on its isotope peak distribution pattern (see inset to Fig. 6(A)). This species is thus attributed to $(2GSH-2H+2Pt+4NH_3)^{2+}$. The spectrum collected after 2 h is shown in Fig. 6(B); another major main product at *m/z* 381.0 is also doubly charged and contains two Pt atoms, and is attributed to $(GSH-2H+2Pt+4NH_3)^{2+}$. At longer reaction times the relative abundance of $(2GSH-2H+2Pt+4NH_3)^{2+}$ decreased while that of $(GSH-2H+2Pt+4NH_3)^{2+}$ increased. The mixture was incubated overnight, and $(GSH-2H+2Pt+4NH_3)^{2+}$ (*m/z* 381.0) was found to be the only species detected in spectra collected 12 h later, as shown in Fig. 6(C). When the mixture was incubated for several days (typically ca. 4 days), a yellow precipitate formed and no species was detected in the mass spectra. Presumably, the product species polymerized after a long reaction time; this behavior has been observed previously by other researchers.[24,28]

The CID spectral data of the precursor $(2GSH-2H+2Pt+4NH_3)^{2+}$ are summarized in Table 4; four ammonia molecules are easily lost sequentially, giving rise to fragment ions at *m/z* 526.5, 518.0, 509.5, and 501.0, respectively. It has been shown in the preceding sections that Pt–N bonds at *trans* positions relative to sulfur are easily cleaved, but that Pt–

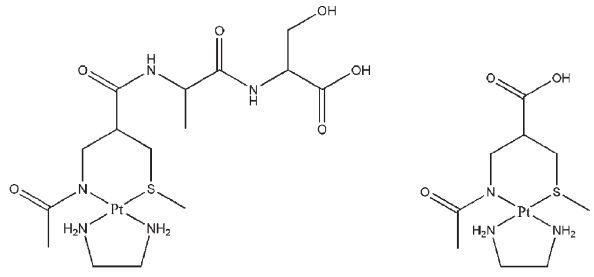

Scheme 4. Structures proposed for $(AcMAS-H+Pt+en)^+$ (left) and $(AcMet-H+Pt+en)^+$ (right).

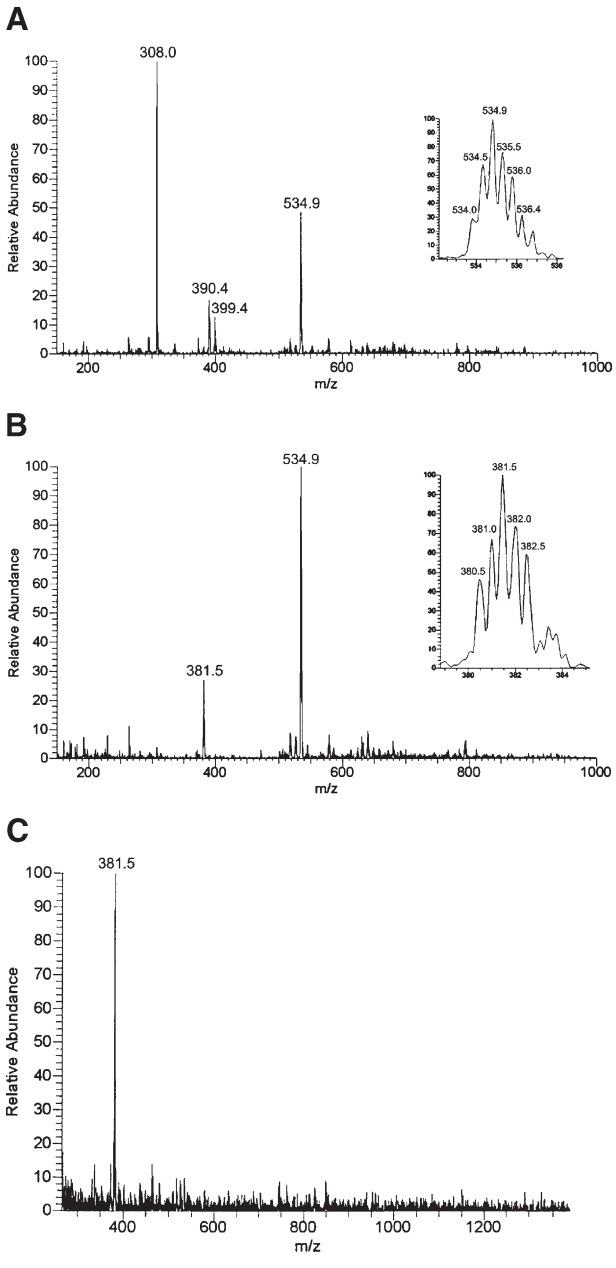

Figure 6. ESI mass spectra recorded after (A) 10 min, (B) 2 h, and (C) 12 h, in reaction of Pt1 with GSH.

Table 4. MS/MS analysis of the precursor ions $(2GSH-2H+2Pt+4NH_3)^{2+}$ (*m/z* 534.9) and $(GSH-2H+2Pt+4NH_3)^{2+}$ (*m/z* 381.5)

Precursor	Fragment *m/z*	Elemental composition	Relative abundance (%)	Assignment
$(2GSH-2H+2Pt+4NH_3)^{2+}$	426.0	$[C_{16}H_{22}N_4O_8S_2Pt_2]^{2+}$	5	$(2b_2-4H+2Pt)^{2+}$
	463.5	$[C_{18}H_{27}N_5O_{10}S_2Pt_2]^{2+}$	5	$(GSH+b_2-3H+2Pt)^{2+}$
	472.0	$[C_{18}H_{30}N_6O_{10}S_2Pt_2]^{2+}$	36	$(GSH+b_2-3H+2Pt+NH_3)^{2+}$
	501.0	$[C_{20}H_{32}N_6O_{12}S_2Pt_2]^{2+}$	22	$(2GSH-2H+2Pt)^{2+}$
	509.5	$[C_{20}H_{35}N_7O_{12}S_2Pt_2]^{2+}$	38	$(2GSH-2H+2Pt+NH_3)^{2+}$
	518.0	$[C_{20}H_{38}N_8O_{12}S_2Pt_2]^{2+}$	100	$(2GSH-2H+2Pt+2NH_3)^{2+}$
	526.5	$[C_{20}H_{41}N_9O_{12}S_2Pt_2]^{2+}$	10	$(2GSH-2H+2Pt+3NH_3)^{2+}$
$(GSH-2H+2Pt+4NH_3)^{2+}$	334.0	$[C_9H_{18}N_4O_4SPt_2]^{2+}$	22	$(GSH-2H+2Pt+NH_3-CO_2)^{2+}$
	355.9	$[C_{10}H_{18}N_4O_6SPt_2]^{2+}$	47	$(GSH-2H+2Pt+NH_3)^{2+}$
	364.5	$[C_{10}H_{21}N_5O_6SPt_2]^{2+}$	100	$(GSH-2H+2Pt+2NH_3)^{2+}$
	372.8	$[C_{10}H_{24}N_6O_6SPt_2]^{2+}$	65	$(GSH-2H+2Pt+3NH_3)^{2+}$

ammonia bonds at *cis* positions relative to sulfur may have moderate stability under CID conditions. Thus it is reasonable to assume that the four ammonia molecules that are readily lost are all at positions *trans* to sulfur. The only possible structure satisfying this assumption is that incorporating four-membered Pt_2S_2 rings, shown in Scheme 5 (top).

The fragment ion at *m/z* 472.0 corresponds to loss of 126 u from the precursor ion, and is attributed to $(GSH+b_2-3H+2Pt+NH_3)^{2+}$. This ion contains one intact GSH, one b_2 fragment from the second GSH, and one NH_3 attached to one Pt(II). Further loss of the remaining NH_3 produced the fragment ion at *m/z* 463.5. The ion at *m/z* 426.0 is attributed to $(2b_2-4H+2Pt)^{2+}$, containing two b_2 residues from the two GSH molecules and all ammonias released. To support this assignment of the fragment ion at *m/z* 426.0, the ion $(GSH+b_2-3H+2Pt+NH_3)^{2+}$ at *m/z* 472.0 was selected as the intermediate ion for MS^3 experiments; the MS^3 spectrum is shown in Fig. 7. It is clear from this spectrum that the ion at *m/z* 426.0 is derived from the precursor ion $(GSH+b_2-3H+2Pt+NH_3)^{2+}$. The ion at *m/z* 454.5 is attributed to simultaneous loss of one ammonia molecule and one water molecule from $(GSH+b_2-3H+2Pt+NH_3)^{2+}$ (*m/z* 472.0). Further fragmentation of $(2b_2-4H+2Pt)^{2+}$ (*m/z* 426.0) via losses of one and two CO molecules gives rise to fragment ions at *m/z* 412.0 corresponding to $(a_2+b_2-4H+2Pt)^{2+}$ and *m/z* 398.0 corresponding to $(2a_2-4H+2Pt)^{2+}$. The absence of fragment ions containing the N-terminus, even in the MS^3 spectra, may suggest that the N-terminal groups of GSH (probably the terminal NH_2) bond to Pt(II) during CID to form a chelate structure that is resistant to further fragmentation.

The CID spectral data for the precursor ion at *m/z* 381.5 are summarized in Table 4. Sequential losses of three ammonia molecules give rise to fragment ions at *m/z* 372.8, 364.5, and 355.9. In contrast with the CID spectrum of $(2GSH-2H+2Pt+4NH_3)^{2+}$, fragmentation of the GSH backbone does not occur. The fragment ion at *m/z* 334.0 corresponds to loss of 95 u from the precursor ion, and this is attributed to loss of three ammonia molecules plus one CO_2 molecule. Therefore, it is reasonable to conclude that the ion at *m/z* 381.5 has a chelate structure that is resistant to backbone fragmentation and contains the free carboxyl group. Based on the structural information revealed by CID spectra, and our proposal that the structure incorporating fused six-membered and five-membered rings also applies to this complex, we propose the structure shown at the bottom of Scheme 5, in

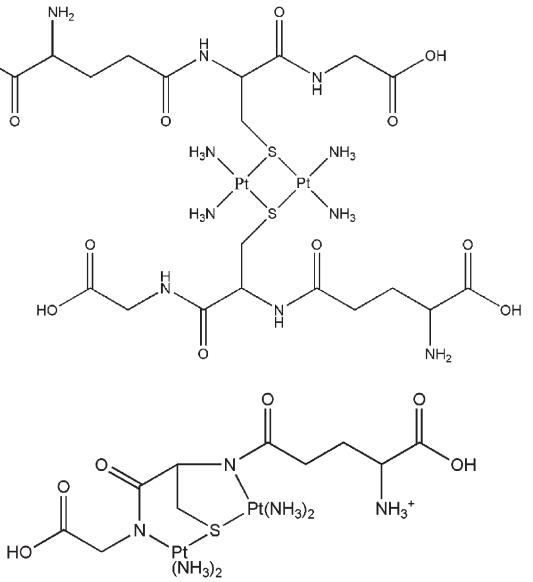

Scheme 5. Structures proposed for $(2GSH-2H+2Pt+4NH_3)^{2+}$ (top) and $(GSH-2H+2Pt+4NH_3)^{2+}$ (*m/z* 381.5) (bottom).

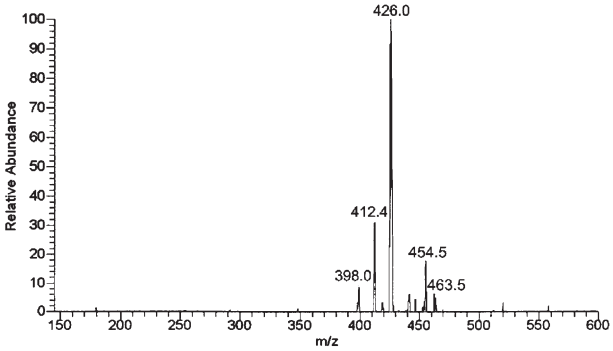

Figure 7. MS^3 spectrum of the precursor $(2GSH-2H+2Pt+4NH_3)^{2+}$ (*m/z* 534.9) via the intermediate ion $(GSH+b_2-3H+2Pt+NH_3)^{2+}$ (*m/z* 472.0).

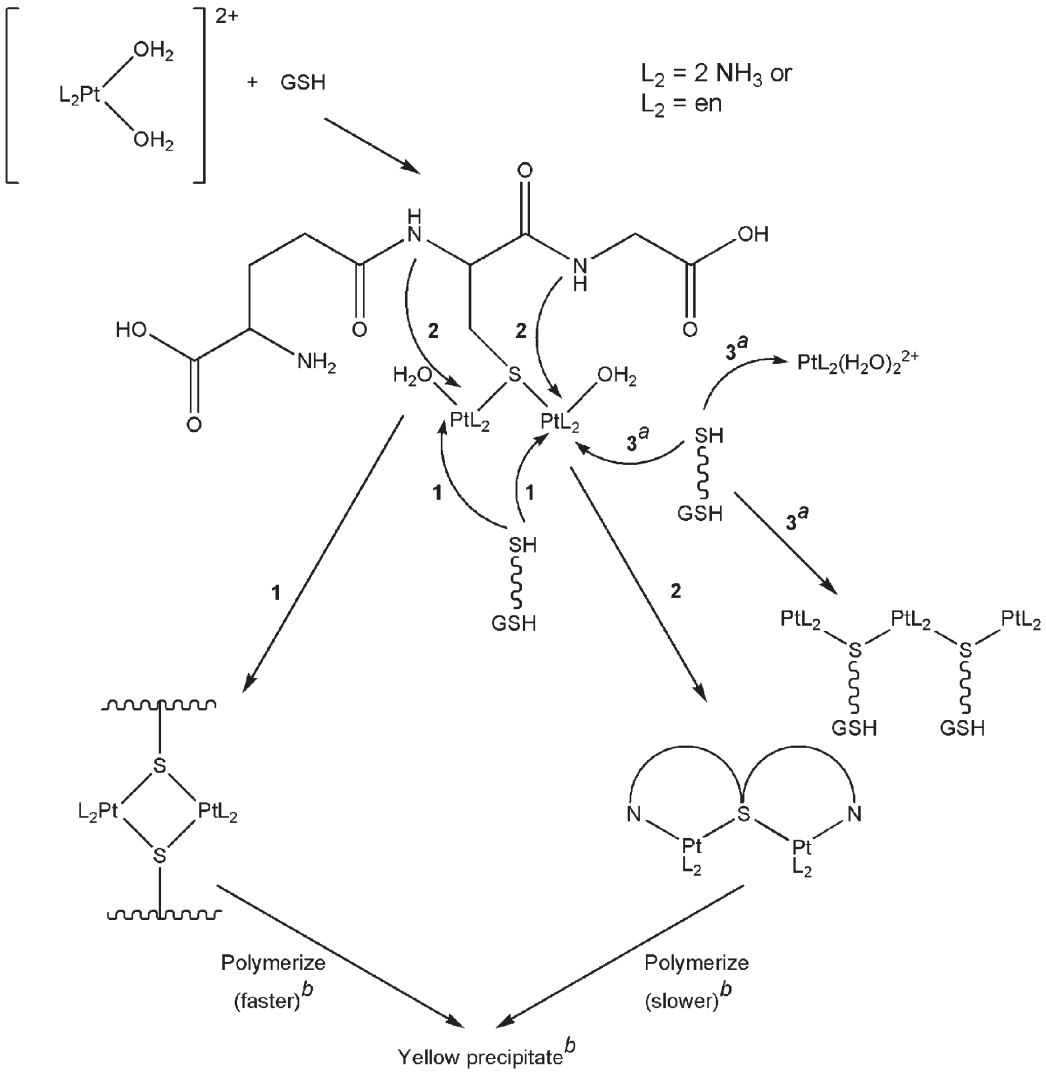

Scheme 6. Proposed reaction pathway for GSH and Pt1 ($L_2 = NH_3$) and for Pt2 ($L_2 =$ en). Processes 1 and 2 are both observed in reactions of Pt1 and Pt2.[a] Process 3 was detected only in Pt2 ($L_2 =$ en) reactions; [b] Process was detected only in Pt1 ($L_2 = 2\ NH_3$) reactions.

which the terminal NH_2 group is protonated (reflecting its basicity).

As shown in the spectrum in Fig. 6(A), at the initial time of the reaction the product at *m/z* 381.5 was not abundant, but two species at *m/z* 390.5 and 399.4 were observed. These two species correspond to complexes of $(GSH-2H+2Pt+4NH_3)^{2+}$ with one and two additional water ligands. Thus the complete reaction pathway for Pt1 and GSH is proposed in Scheme 6 ($L_2 = 2\ NH_3$).

Reaction of Pt2 with GSH was much slower than that of Pt1. The mixture was incubated for more than 12 h, after which the reactant GSH still remained as the predominant species, i.e. products were considerably less abundant than the reactant. A typical spectrum collected after ca. 6 h is shown in Fig. 8. The ions at *m/z* 407.6 and 561.2 are doubly charged species, attributed to $(GSH-2H+2Pt+2en)^{2+}$ and $(2GSH-2H+2Pt+2en)^{2+}$, respectively, and the ion at *m/z* 687.7 is attributed to $(2GSH-4H+3Pt+3en)^{2+}$. It is reasonable to propose that $(GSH-2H+2Pt+2en)^{2+}$ and $(2GSH-2H+2Pt+2en)^{2+}$ have structures similar to those of their Pt1 counterparts. The difference in reactivity presumably arises from the structural difference between Pt1 and Pt2; the five-membered chelate ring in Pt2 causes considerable steric hindrance when forming fused chelate rings with the coordinating groups of GSH. Due to this hindrance, formation of a Pt_2S_2 four-membered ring is relatively unfavored and so $(2GSH-4H+3Pt+3en)^{2+}$, which has a Pt–S–Pt–S–Pt linear structure, is formed instead. The corresponding species was not observed in the reaction of Pt1 with GSH. Unfortunately,

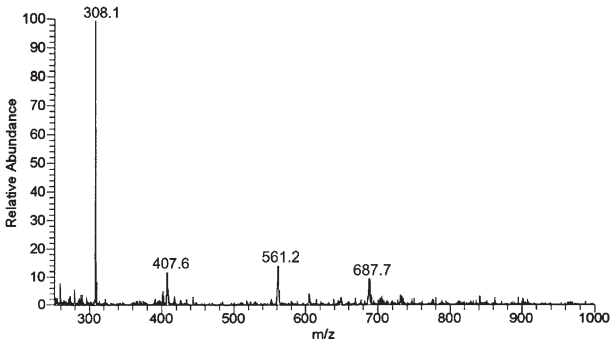

Figure 8. ESI mass spectrum recorded after 6 h in reaction of Pt2 with GSH.

CID spectra could not be recorded for this ion due to its low abundance. The reaction pathway proposed for Pt2 plus GSH is also shown in Scheme 6 (L_2 = en).

CONCLUSIONS

The present results have demonstrated that ESI-MS can be used as an effective tool to study interactions between platinum(II) complexes and peptides. ESI-MS can provide a qualitative picture of the composition of the pre-sprayed solution, and some important reaction parameters of similar reactions, e.g. relative reaction rates, can be intuitively obtained. CID spectra can provide valuable structural information. The structures deduced from CID analysis are generally in good agreement with those derived previously from other experimental techniques such as NMR.

Pt1 and Pt2 are shown to have different reactivities toward some peptides, although the structures of the formed complexes are generally similar. In some cases they form complexes with different chelate structures, and these differences are attributed to steric effects caused by the chelating ligand en in Pt2. Ligand ammonia molecules located at *trans* positions relative to sulfur are usually easily lost, mainly due to the strong *trans* effect of sulfur, while loss of the bidentate ligand en is less favored compared to ammonia.

Due to its great medical, biological and biochemical importance, platinum chemistry is attracting considerable interest. Using ESI-MS and MS/MS techniques, in conjunction with other analytical methods, extension to the study of interactions of other platinum complexes with longer peptides, proteins or other biomolecules will provide new insights into this active research area.

Acknowledgements

This work was supported by the National Science Foundation of China (Nos. 20271027 and 20231010).

REFERENCES

1. Lippert B. *Cisplatin, Chemistry and Biochemistry of a Leading Anticancer Drug*. Wiley-VCH: Weinheim, 1999.
2. Howell SB. *Platinum and Other Metal Complexes in Cancer Chemotherapy*. Plenum Press: New York, 1991.
3. Lempers ELM, Reedijk J. *Adv. Inorg. Chem*. 1992; **37**: 175.
4. Milovic NM, Dutca LM, Kostic NM. *Chem. Eur. J*. 2003; **9**: 5097.
5. Zhu L, Kostic NM. *Inorg. Chem*. 1992; **31**: 3994.
6. Sun X, Jin C, Mei Y, Yang G, Guo Z, Zhu L. *Inorg. Chem*. 2004; **43**: 290.
7. Liu Q, Wei H, Lin J, Zhu L, Guo Z. *J. Inorg. Biochem*. 2004; **98**: 702.
8. Colton R, James BD, Potter ID, Traeger JC. *Inorg. Chem*. 1993; **32**: 2626.
9. Loo JA. *Mass Spectrom. Rev*. 1997; **16**: 1.
10. Carr SA, Hemling ME, Bean MF, Roberts GD. *Anal. Chem*. 1991; **63**: 2802.
11. Cohen P, Gibson BW, Holmes CFB. *Methods Enzymol*. 1991; **201**: 153.
12. Light-Wahl KJ, Springer DL, Winger BE, Edmonds CG, Camp DG, Thrall BD, Smith RD. *J. Am. Chem. Soc*. 1993; **115**: 803.
13. Doktycz MJ, Habib-Goudarzi S, McLuckey SA. *Anal. Chem*. 1994; **66**: 3416.
14. Colton R, D'Agostino A, Traeger JC. *Mass Spectrom. Rev*. 1995; **14**: 79.
15. Aliprantis AD, Canary JW. *J. Am. Chem. Soc*. 1994; **116**: 6985.
16. Henderson W, Nicholson BK, McCaffrey LJ. *Polyhedron* 1998; **17**: 4291.
17. Dhara SC. *Indian J. Chem*. 1970; **8**: 193.
18. Biemann K, Martin SA. *Mass Spectrom. Rev*. 1987; **6**: 1.
19. Loo JA, Hu P, Smith RD. *J. Am. Soc. Mass. Spectrom*. 1994; **5**: 959.
20. Luo X, Huang W, Mei Y, Zhou S, Zhu L. *Inorg. Chem*. 1999; **38**: 1474.
21. Luo X, Chen X, Song Y, Zhu L. *Chem. Lett*. 1998; 1079.
22. Reiter A, Adams J, Zhao H. *J. Am. Chem. Soc*. 1994; **116**: 7827.
23. Hu P, Loo JA. *J. Am. Chem. Soc*. 1995; **117**: 11314.
24. Appleton TG. *Coord. Chem. Rev*. 1997; **166**: 313.
25. Hahn M, Kleine M, Sheldrick WS. *J. Biol. Inorg. Chem*. 2001; **6**: 556.
26. Wolters D, Sheldrick WS. *J. Chem. Soc., Dalton Trans*. 1999; 1121.
27. Schaaff TG, Qu Y, Farrell N, Wysocki VH. *J. Mass Spectrom*. 1998; **33**: 436.
28. Appleton TG, Connor JW, Hall JR, Prenzler P. *Inorg. Chem*. 1989; **28**: 2030.